A comparative study of natural Tunisian clay types in the formulation of compacted earth blocks

S. Mkaouar, W. Maherzi, P. Pizette, H. Zaitan, M. Benzina

A comparative study of natural Tunisian clay types in the formulation of compacted earth blocks

Safa MKAOUAR [1, 2 *], Walid MAHERZI [2], Patrick PIZETTE [2], Hicham ZAITAN [3] and Mourad BENZINA[1]

[1]Laboratory "Water, Energy and Environment" (LR3E), National Engineering School of Sfax, University of Sfax, Tunisia.

[2] IMT Lille Douai, Univ. Lille, EA 4515 - LGCgE - F-59000 Lille, France.

[3]Laboratory "Chemistry of Condensed Matter" (LMCC), Faculty of Science and Technology Fez, University of Sidi Mohammed Ben Abdellah, Morocco.

*Corresponding author

E-mail address: safa_mkaouar@yahoo.com

Abstract

This study investigates the physico-chemical, mineralogical and thermal characteristics of three natural Tunisian clays collected from Gafsa (A1), Zeramdine (A2) and Nabeul (A3). The aim was to promote an appropriate formulation of materials and to obtain optimal compacted earth blocks (CEB). Results of mineralogical analysis of clays revealed the dominance of kaolinite (> 13.58%), illite (>25.7%), quartz (> 18%) and a minor fraction of smectite phases. Chemical analysis of the clays major elements showed a SiO_2 content exceeding 50% and a percentage of Al_2O_3 higher than 18%. Particle size distribution showed that clay fractions varied from 10 to 20 %. Plasticity index defined a plastic character while the values of specific surface area were around 60 m^2/g. This discrepancy has an effect on the behavior of these clays in CEB, notably their mechanical properties. From this characterization, it appears that all the sampled clays are suitable as raw material for CEB application. The prepared CEB formulations varied according to compaction energy and binder dosages. In this work, lime served as a binder at different rates (4, 6, 8 and 10%) to ameliorate the quality of CEB. Unconfined Compressive Strength values were determined by Static method test. Then bulk density, shrinkage and porosity values of samples were

determined. Compressive strength could reach 7 MPa with lime supplementation in sample A1. The static compaction onto the sand-clay mixture achieved a value of density superior to 2 $g.cm^{-3}$ with lime supplementation in sample A1. Overall, the Gafsa clay was the most suitable for CEB preparation. Also, lime improved the compressive strength of the matrix, in addition to its ecological merits.

Key words

Clay, physico-chemical characterization, compressed earth blocks, lime, packing density, compressive strength.

Highlights

* Tunisian clays from Nabeul, Zeramdine and Gafsa were investigated
* An ecofriendly and optimal CEB formulation was sought.
* Mixtures preparation influences physical and mechanical properties of CEB
* Lime use as a binder improves mechanical properties of CEB.
*Correlation could be established between porosity, shrinkage, packing density and strength of the CEB.

1. Introduction

The production process of fired clay bricks has a considerable negative impact on the environment [1]. This implies significant production costs, due to fuel prices and huge CO_2 emissions in the nature that contribute to increased greenhouse effects which leads to global warming [2]. Therefore, the need to produce low-cost and eco-friendly construction materials has become a major concern [3, 4]. Developing new sustainable building materials is a prime consideration in the preservation of the environment [4, 3]. In fact, the harmful impact of building materials on the environment must be reduced throughout their life cycle. New technologies based on optimizing the choice of raw materials play an important role in this approach by using ecological, local and renewable materials. In particular, earth is considered the oldest source of building materials with low acquisition cost. A more ecological alternative to the common fired clay brick is the compressed earth block (CEB) [1]. Interestingly, this building material has attracted much interest and several attempts to optimize its formulation have been made. Morton indicated that CEB could win more than 80% of energy compared with fired clay brick [5].

Tunisia is endowed with an abundance and diversity of geological clay minerals. In this context, some Tunisian clays were the objective of this study. Materials from three Tunisian sites were characterized and tested for CEB formulation at different clay/sand proportions. Also, lime was used as a binder and the mechanical strength of the different matrices were compared.

2. Materials: Geological setting

Three different clay samples were used in this study. The first sample was collected from Djebel Bouamrane "Gafsa" located in Southwest of Tunisia. This clay is red and belongs to the Turonian age and Beida formation. The second clay was obtained from Zeramdine quarry (Jemmel) "Monastir" in the Northeast of Tunisia. It is a white clay of Serravallien-Totonian age and Oum Douil formation. The third one was brought from Djebel Abderrahmane "Nabeul" (situated in Northeast of the country). This type of clay is green, of Serravalian age and Souaf formation. Samples were tagged A1, A2 and A3, respectively as represented in Fig. 1. At first sight, it appears clearly that the main difference between these three types of clays is due to their origin. The composition and structure of clays depends on their origin as well as geology of the location.

After extraction, each sample was grinded and dried in an oven at 60°C until a constant weight was reached.

In this present study, clay deposits were identified and characterized in terms of their physicochemical, mineralogical and morphological properties.

3. Methods

3.1. Materials identification and characterization

Samples were characterized by several chemico-physical methods, which allowed us to classify and compare clay characteristics and behaviors. Grain size analysis determines the particle distribution of samples and allows to classify the materials according to their Constituent parts (clay, sand, gravel). This test was performed to standard 13 320-1 and using Coulter LS 13 320 Laser device and Fraunhofer 780d optical model. The detection particles size was range from 0.375 µm to 2 mm.

Casagrande method describes the samples plastic behavior by the determination of Atterberg Limits. Liquid limit (LL), plastic limit (PL) and plasticity index (PI) were determined according to standard NF P 94-051 (1993) and GTR-LCPC (1987) [7, 8]. Specific gravity G_s of solid grains was determined using an AccuPyc 1330 helium gas pycnometer.

Chemical composition of the clay was determined using Brucker S4 based on X-Ray Fluorescence spectrometry measurements. Loss on ignition consists on placing samples in a furnace with temperature of 550°C for 3 hours to determine its mass loss. Volatile substances lost consist of molecular water carbon dioxide from carbonates and the presence of organic matter.

$$\text{Percent LOI} = ((\text{wet weight} - \text{dry weight}) / \text{dry weight}) * 100$$

Mineralogical composition of the clay samples was determined by X-Ray-Diffraction using an Advance Bruker AXS D8 energy dispersion diffractometer to determine the mineral phases in the material. This method concerns analyzing raw powder clay and randomly oriented preparation: air-dried (at room temperature), saturated with ethylene glycol (EG) and heated to 550°C for 1 h of the clay fraction after centrifugation. The preparation of oriented blades was performed according to Moore and Reynolds, 1997 [9].

Specific Surface Area and pores volume of samples were obtained by azote adsorption isotherms methods at -196°C using a Micromeritics BET ASAP 2010 sorptometer. Morphological features of the clays were analyzed by a Scanning Electron Microscope Hitachi S-3600N apparatus.

Thermo-Gravimetric-Analysis (TGA) was performed by a Nestzsch STA 449F3 instrument and the weight loss in function of temperatures between 105°C – 1000°C was recorded.

3.2. Mix design of CEB

The principle and the process of CEB production consists of using raw material compacted and mechanically shaped. In order to evaluate the compaction properties of representative clays, various compression tests were carried out. The test consists of mixing and homogenizing all dry components (clay, sand, lime), and then a sustainable amount of water is added to manufacture the paste of bricks. Obtained mixtures were extruded into cylindrical test specimens (50 mm of diameter and 100 mm of high).

Pressure of 20 MPa allows to compact mixture using a specific mold in order to obtain homogeneous and well stabilized samples. Unconfined Compressive Strength (UCS) was measured according to standard NF P 98-232.1 [11], using an Instron 300 DX model-testing machine, connected to a Partner TM Testing Software. Failure of test piece makes the end of UCS test; ramp speed used was 11.78 kN/min. Stress and strain were automatically registered. Compaction used for specimens was static compaction with simple effect type, ensured by means of a hydraulic press. The lower plate of press moves while the assembly (mold + mixture + piston) and the upper plate remains fixed. The operation was conducted until desired compaction stress is reached. During all stages of this study, mixtures were subjected to a compaction stress of 20 MPa. After demolding test pieces, the diameter, height and mass of each specimen were immediately measured. After shaping, a drying phase in furnace at 60°C for 7 and 28 days was necessary, in order to remove residual water in the produced bricks. Subsequently, molds manufactured were subjected to different mechanical tests [12].

During this work, an experimental study of raw earth materials behavior was carried out. Two formulation steps were studied: (a) the first was to look for granular matrix (mixture composition) in order to achieve the most effective mechanical resistance. (b) The second was to study mechanical properties reinforced by adjuvants. This additive allows to improve final product properties. Indeed, lime stabilization is a process that chemically improves many characteristics of soils especially compressive strength. The influence of several parameters has therefore been tested on mechanical behavior of the products obtained.

4. Experimental Results

4.1. Characterization of raw clay samples and position with respect to CEB recommendations

4.1.1. Particle size distribution data

Particle size distribution presents one of the main criteria in manufacturing suitable earth blocks. Fig. 2.a shows the particle size distribution of natural clay, sand as well as the recommendation range deduced from the CEB norms NF XP P13-901[13].

Granulometry curve of natural clay was beyond the range because they were much finer. Thus, sand 0/ 2 mm was added. Data obtained showed that the new granulometry curve of mixture was well positioned on the recommendation range (Fig. 2.b).

Table 1 presents the composition of cohesive soil for three samples. Results show that 13.77, 19.62 and 9.62 % of Clay, 58.14, 46.48 and 27.7 % of silt and 28.09, 33.9 and 63.11 % sand compose samples A1, A2 and A3, respectively. Therefore, sample A3 had the coarsest fraction. The presence of high fraction of silt gives the material an importance for the construction field. This fine fraction given by clay plays an interesting role in building as it fills the voids created by the sand (coarse fraction), resulting in a denser mix [2].

The sand formulation used comprises 2.07% clay, 6.72% silt and 91.21% sand. Fineness modulus of sand is 2.29, which characterizes an optimal sand referring to NF EN 933-1 (2.2 <Mf <2.8) [14].

According to results (Table 1) revealed by the curvature coefficient Cc and Cu (1<Cc<3 and Cu <2). These materials are dense, well graduated and have uniform particle size [15, 16].

Helium pycnometer method confirms geotechnical results, the sample A1 (ρ = 2.77 g.cm^{-3}) was denser than A2 (ρ= 2.63 g.cm^{-3}) and A3 (ρ=2.57 g.cm^{-3}). The density of the sand used is 2.65 g.cm^{-3}.

4.1.2. Atterberg limits

Fig. 3 show the plasticity chart by Casagrande and the plasticity index that is represented in the diagram proposed by norm NF XP P13-901. Low swelling behavior characterized A1 and A2 samples. Therefore, these clays A1 and A2 are considered non-plastic, in the way it is easy to dry and have a good optimization of block fabrication. Soils A1 and A2 had a low plasticity index value, which indicates their low clay content and the abundance of quartz.

Results also show that these clays have low shrinkage that is appropriate for blocks production (W_r< 12) [7, 8]. Soils can be considered, according to plastic index, as solid state (W <W_p, I_c>1, II < 0) for all samples.

4.1.3. Chemical identification

Chemical analysis indicates that samples were rich in silica, alumina and alkalis. The SiO_2 content was up to 50% (m %) in all studied samples, as the Al_2O_3 values ranged from 18 to

20% (wt %). As shown in Table 2, mass ratio SiO_2 / Al_2O_3 values are higher than the classic value founded in pure kaolinite (SiO_2 / Al_2O_3 = 1.18) and montmorillonite (SiO_2 / Al_2O_3 = 2.36) [17]; due to the quantity of quartz present. Lime content was reactively low in all samples that confirm current objectives and CEB production. This amount was high for clay A3 (calcium clay). According to Jamoussi et al., 2003[18], the clays have high content of K_2O ranging between 2.53and 6.38% due to the presence of illitic phase.

Loss on Ignition (LOI) is determined by calcination powders up to 1000°C. The high LOI was associated to the presence of carbonates and the bound water evaporated by heat treatment. This result explains the test water content of each sample, as well as the large capillary retention due to its large surface area. LOI content values were 5.07, 6.42 and 12.24 for samples A1, A2 and A3. It is noted that clay A3 was the wettest. These high content values can be explained by a significant proportion of kaolinite.

4.1.4. Specific surface area analysis

Nitrogen adsorption-desorption isotherms recorded on the clay materials (A1, A2 and A3) are presented in Fig. 4. For these representative clays, isotherms were of type IV isotherm according to the IUPAC classification, which is characteristic of porous adsorbents having pore sizes in the range of 70-100 Å [10, 19]. The superposition of adsorption and desorption curves shows the absence of internal mesoporosity of the sample, especially for clay A1. The presence of internal and inter-granular pores and the hysteresis is explained by the internal porosity of the material. Indeed, the more the number and the pore size increases, the specific surface area becomes higher [10, 20].

Values of specific surface area vary between 22.46, 63.4 and 64.22 m^2/g for A1, A2 and A3 samples, respectively. The sample (A1) had a smaller specific surface than A2 and A3, due to its microstructure. Type of clay, minerals associated and the dominance of illite and kaolinite phases influenced the results [18].

Consequently, with Pycnometer test, values of porosity and porous volume are in agreement with the precedent analysis. The internal porosity values were of 50.46, 44.37 and 38 % for A1, A2 and A3, respectively. The porous volumes are 0.37, 0.35 and 0.29 $cm^3.g^{-1}$ for A1, A2 and A3, respectively.

4.1.5. Optical microscopy and SEM characterization

Optical microscopy and SEM allow observing the sample surface's topography; it provides detailed surface data of solid samples. Fig.5 displays textural characteristics of clay samples obtained by SEM analysis. SEM images show that the samples A2 and A3 have a

discontinuous structure and an open texture with the presence of visible and connected voids. Soil A1 presents a compacted microstructure, with the presence of a porous structure, which could provide a high value of porosity and a high adsorption capacity. Clay A3 contains the coarse fraction compared with A1 and A2.

4.1.6. Mineralogical identification

The mineralogical structure of various natural clay samples was studied [9, 21]. According to Fig. 6, Kaolinite, illite and smectite are the main clays present in the materials.

The centrifugation technique allows separating minor fraction from each sample. Samples placed into oriented blades were scanned in air-dry state, treated by glycol solvation and heated at 550°C. The most mineralogical phases identified were Illite, Kaolinite, Smectite and Quartz.

The presence of kaolinite phase was confirmed by the presence of the reflection at 7 Å (powder) and that disappears after heating at 550°C: kaolinite is transformed into metakaolin above 450°C. Smectite was clearly identified by comparing diffraction patterns of air-dried and ethylene glycol EG solvated. Kaolinitic phase contributes to good drying characteristics of materials [4]. The mineralogical composition of the clays consisted of 13.58% Kaolinte (K), 25.7 % illite (I), 11.82% smectite (S) and 48.90% quartz (Q) and impurities for A1. The clay A2 is composed of 25.3 % K, 45.83 % I, 38.9% S and 24.98 % Q, while A3 is formed by 38.34 % K, 24.89 %I, 18.74 %S and 18.03% Q.

Kaolinite is the most used mineral for CEB manufacture. Quartz is always associated with kaolinite. The presence of kaolinite minerals contributes to good shaping, ameliorates plasticity properties and limits the drying properties. In contrast, Smectite phase increases moisture content as shown in sample A3. This contributes to shrinkage phenomena [21]. The soil A1 is composed of a high rate of quartz that explains low plasticity as demonstrated.

4.1.7. FTIR analysis

The infrared spectrum shows the presence of several characteristic absorption bands in the infrared region 4000 to 400 cm^{-1}. Results are shown in Fig. 7. The identification of soil minerals by FTIR analysis is determined by reference to spectra (Farmer, 1968) [18, 23, 24].

FTIR spectra patterns showed heterogeneous mixtures of clay components and differences in their composition and structure. First, infrared absorption properties of kaolinite corresponding to OH bands were established at 3563.33 cm^{-1} for A1, 3624.15; 3611.79 cm^{-1} for A2 and 3645.37 cm^{-1} and 3611.79 cm^{-1} for A3. In addition, specific bands of accompanying mineral were observed (presence of kaolinite form and quartz) at 952.32 cm^{-1}

for A1, 974.69 and 687.69 cm^{-1} for A2 and 989.60, 907.60 and 687.69 cm^{-1} corresponding to clay A3. The quartz was detected at 775.28, 780.87 and 777.14 cm^{-1} for A1, A2 and A3 respectively. The band at 1625.12 cm^{-1} for clay A2 is attributed to the presence of an amorphous alumino-silicate OH group. These results confirm and corroborate the XRD data.

4.1.8. TDA/TGA analysis

Water evaporation and carbonate decomposition are the most significant weight loss processes in CEB manufacturing. According to research work of Aras and Farmer [21, 23], thermal analysis of raw materials and weight loss represented in Fig. 8 could be due to the same process.

In clay materials, some reactions are responsible for mass loss as H_2O and organic materials. A first endothermic peak was depicted at low temperature (< 150°C for all clays studied); this loss is attributed to moisture elimination and absorbed water departure, and consequently the loss of weakly bound water. Mass loss around 520°C is due to the removal of water content from clay minerals indicating the dehydroxylation reaction. The decomposition of carbonates (740 °C) was detected only in the structure of clay A3.

Total weight loss of A1, A2 and A3 were 4.7 %, 8.69 % and 14.51 % respectively (Fig. 8). The greatest mass loss was obtained in sample A3; which is in a good agreement with its chemical and mineralogical composition (LOI and alkaline oxides content).

Moisture or water contents can be directly measured using a known volume of the material, and a drying oven. Values obtained were 2.47, 4.3 and 7.46 for A1, A2 and A3, respectively.

Results based on mineralogical, chemical and physical characteristics, show that the raw clays studied display an interesting potential for CEB.

4.2. Potential application

The influence of several parameters was tested on the mechanical behavior of the products obtained. For three types of clay selected, it was interesting to study different factors: water content, mixture composition and setting time, in order to evaluate the variation of mechanical properties and achieve the optimal compressive strength. Table 3 summarizes the formulations and the quantities of materials used for each block series.

After remolding test pieces, some blocks presented a heterogeneity on their surface due to the difference of mixture constituent's particle sizes (Fig. 9). After drying for 7 days, none of the blocks, even with calcined clay A3 had a trace of efflorescence, an aesthetic problem due to the presence of white spots on the surface of specimens.

The clay behavior under static compaction test was used in order to study the impact of compression load on compacted earth properties. The compaction energy is an important element in static compression test. This process measures the amount of energy based on properties of soil and the amount of water content. Mechanical behavior of blocks in compression was characterized through displacement-controlled uniaxial tests (Fig.10 (a), 10 (b)).

Displacement in compression (dh) for wet soil is shorter than dry soil. Indeed, a soil with high water content reaches dh faster compared to low water content. Water content influences sample displacement in mold test tube height. So, increasing water content fosters the saturation of soil, (Fig. 10 (a)), therefore pores are saturated and pore volume is reduced during compaction (Fig. 10 (e)). Lime addition into materials consumes much time (difficulty of settlement) to be compacted than untreated samples (Fig. 10 (b)). Displacement in compression of sample with lime is slower: lime densifies the material, flocculates and coagulates clays, then absorbs water and fills voids (Fig. 10 (f)). However, the variation remains associated with the type of clay and differs according the character of swelling. That is why it shows some differences in the three types of soils especially soil A3 that contains an important percentage of smectite phase minerals.

The mechanical behavior of blocks in compression was characterized through displacement-controlled uniaxial tests and behavior curves (stress-strain). Fig. 10 (c), 10 (d) shows the behavior of material defined by two states: a linear state and a softening state. For weak deformations, a linear elasticity and a rigid behavior characterize the materials. The pre-peak region is relative to small deformations compared to total deformation. The post-peak region called softening zone results in a loss of bearing capacity of specimen without thereby fragmentation. It is remarkable that the peak or maximum of shear stress corresponds to the fracture of specimens. Beyond the peak (ultimate strength), stress decreases, then there is an inflection point of post-peak curve where deformations become significant compared to stress drop Fig. 10 (c), 10 (d). Strong materials (with low water content and with lime added) can support high tensile force compared with weak materials that broke very quickly as presented in Fig.10 (e), 10(f)). Addition of lime makes the blocks more resistant [26, 27, 29].

Density is the key indicator used to classify solid construction blocks. Compressive strength of earth blocks samples depend on their density. After compacting final height (Hf) and wet mass (Mh) of test pieces are measured. These data allow calculating dry density of specimen. A material with high water content needs less energy to achieve the same dry density (γ_d)

since water plays the role of lubricant. Compacting wet soils consumes less energy compared to dry one, as the frictional dissipation is more important. As water content increases, saturation of soil increases and therefore pores are saturated and pore volume is reduced during compaction.

The rate of adjuvant increases samples' density as presented in Fig. 11. The increase in maximum dry density is a reliable indicator of clay improvement. Results demonstrate that the weight of samples fell remarkably high, due to the increasing number of voids formed within blocks by the highly porous clay particles. Increase in density is attributed mainly to the filling of voids between soil particles and natural pozzolan as the latter has a higher specific gravity.

Most of density values obtained were justified by Delebecque R and Guilaud H [29, 30]; in the range of 1.7 and 2.2 $g.cm^{-3}$ (Fig. 11). The maximum dry density acquired was due to particle size and specific soil surfaces.

For the production of CEB, the specimens were tested and characterized at a laboratory test. Weight loss, drying shrinkage, porosity, packing density as well as the compressive strength were determined.

4.2.1. Weight loss

Mass loss is due to departure of added water. It is calculated from the following formula.

$$LM = (M_i - M_f / M_i) * 100$$

M_i: Initial mass before drying

M_f: mass after drying

Table 4 presents the result of weight loss of samples. Increasing water content leads to further mass loss. In fact, the material becomes wetter and then excess water is released. Mass loss increases with also setting time because an important amount of water evaporated. Therefore, with more drying time in the oven, material still loses its mass and becomes more resistant (Table 4 a).

Mass loss for clay A3 was more important than A2 and A1; this result is related to chemical analysis, loss on ignition, moisture content and TGA curve analysis (heat release and H_2O peaks). A3 also contains a high quantity of smectite and requires significant water content.

Lime addition makes mass loss very important. In fact, lime closes pores and fills voids. Decreasing void rate between grains makes resistance rather significant and hence the

mechanical strength (Table 4 b). To conclude, soils A1, A2 and A3 have a different behavior depending on the moisture content.

Fetra et al (2016) confirmed this result and explained it by high porosity of hydraulic lime that allows excess moisture to be released instead than stores it inside. Excess moisture captured inside materials in building is unhealthy. In fact, we use hydraulic lime for the simple reason of allowing building to 'breathe' [31].

4.2.2. Drying shrinkage

Drying shrinkage is a key parameter in measuring the quality of the CEB. It reflects an expansion/contraction behavior. The test is responsible on the capacity of clays to release or store water [32]. The drying step is very important as it avoids cracking of the samples. According to the results obtained (Table 4), the shrinkage percentage depends on clay type and give us an idea about the important amount of water evaporated [32]. High shrinkage value are disturbed for clay rich in $CaCo_3$. In fact, volumetric shrinkage depends on flux materials, the percentage of mixing water and the decomposition of gaseous phases. Flux materials could fill voids and compress between spaces, in against part, gases generated could be generated pores [33].

The shrinkage value of the manufactured blocks decreased linearly with the lime supplementation (Table 4 b). This is due to the increase in the initial moisture content present in the clay mixture with the lime addition. Thus, obtained product incorporated with lime could be further evaporated because of the organic matter present, which causes the expansion phenomenon and lower shrinkage.

4.2.3. Porosity and packing density

Understanding the behavior of a mixture requires the knowledge of its packing density. Data of porosity and packing density are shown in Table 5, where the sum of porosity and compactness is equal to 1. The ratio between absolute density and bulk density refers to compactness.

Porosity affects significantly the mechanical properties, durability, and water absorption. A high water content leads to increasing porosity and the structure becomes less compact and less dense. Lime, due to its porous character, allows to fill voids, then densifies the material and increases its packing density.

Generally, organic matter decomposition generates small pores in the matrix. Fluxing agents (Fe_2O_3, K_2O, MgO, CaO and Na_2O) play a key role in the porosity [33, 34]. Sources of fluxing agents like K_2O, Na_2O_3 and Fe_2O_3 allow densifying clay. As shown in clay A1 and

A2, important values of flux materials (K_2O, Na_2O_3 and Fe_2O_3) compared to clay A3 led to the densification of particles, thus particles close together. Besides, for A3, high content of CaO and MgO act as pore generating agent. Therefore, increased porosity was observed for specimens leading to decrease of mechanical strength properties. Table 5 show some differences in values of porosity of three types of soil studied. The different values of porosity are also due to the amount and size of pores. In conclusion, as shown, less void volume (reduced porosity) was associated with compact and dense structure, higher strength and therefore better quality.

4.2.4. Mechanical strength

Compressive strength is the most important parameter of construction blocks. Compression tests were carried out using an ISTRON type mechanical press (the same used during the testing of specimens).

- Mixture composition effect

The difference in compressive strength is very clear and varies with different raw material rates. Indeed, for a maximum resistance, the optimum mixture chosen was 70% sand / 30% Clay (tab. 6).

- Water content effect

According to data collected, unconfined compressive strength for specimens cured after 28 days are higher than after 7 days as presented in Fig. 12. For different mixtures prepared, it can be seen that an increase in water content caused a decrease in the compressive strength values after 7 and 28 days. Indeed, the presence of water in specimens weakened their resistance. Furthermore, water content was evaporated with the setting time, so compressive strength increased. Setting time allows occupying and filling voids and pores into blocks creating then a dense structure. The less void volume is related with higher strength and therefore better quality [35, 36, 37].

- Effect of lime added

Stabilizing soil is very important in manufacture of CEB in order to ensure good mechanical properties. In general, lime can be an excellent choice to treat soils. The advantage of this stabilizant is related to its low quantity added and its ecological use. The reaction between lime and clay produces stable calcium silicate [2].

A Natural Hydraulic Lime NHL with 3.5 MPa (moderately hydraulic) was used; this type of hydrated lime is highly required for soil stabilization. The hydraulic lime properties has characterized by a slow setting time and a good compressive strength [36]. Hydraulic lime is

recommended because it allows absorbing carbon dioxide from air and having low plasticity that hinders the formation of cracks [38].

According to data obtained (Fig. 13), values of compressive strength are better for stabilized soil with lime compared with untreated soil. The addition of lime as adjuvant improves mechanical properties of the material. Lime slow reaction and the quality of earth explained this result [39, 40]. Values of compressive strength obtained are in correlation with some researches such as Delebecque R and Guilaud H [26, 27].

To conclude, there are two main modes of lime treatment to improve performance of earth materials, which are structure modification and stabilization. In fact, these modes can upgrade mechanical strength of soils. In the first reaction, the process makes the flocculation and agglomeration of clay minerals leading to a reduction in plasticity and moisture content. This phenomenon also contributes to changing clay texture and improves consistency of treated clay soils.

Lime dissolution in soil allowed the saturation of calcium. Clays released alumina and silica that react with calcium to form calcium hydrates CSH. A pozzolanic reaction and a cementitious product were formed with good mechanical properties. Adding lime to a reactive soil formed stable calcium silicate hydrates CSH that in turn explain the increase of resistance. Then, mixing lime with clay caused hydration of clay particles by fixing a quantity of water to make a more granular and resistant structure [31, 39, 40].

Lime effect was very dependent on nature and type of clay used. In fact, compressive strength was a function of clay variety. In fact, lime reacts much faster with montmorillonite clays than with Kaolinite, thus reducing plasticity for the first and having little effect on the plasticity of Kaolinites. Lime modification showed increase in strength for expansive (kaolinite) better than expandable clay (montmorillonite) [37]. In view of this, we can conclude that an increase in compressive strength is a function of setting time and the proportion of lime added. The mechanical behavior of the blocks depends on the granulometry, type of clay, water contents and binders. Compressive strength of blocks depends also on their density, porosity and pore size distributions.

5. **Conclusion**

In this paper, three clays sampled from different geographical locations (Djebel Bouamrane Gafsa, Zeramdine quarry and Djebel Abderahmanne Nabeul) were studied. Mineralogical analysis of samples indicated the presence of illite and kaolinite as dominant mineral phases

associated with smectite and quartz. The behaviors of clay bricks depended on the nature, type and the amounts of various minerals present and physico-chemical analysis.

Results for manufacturing bricks and Unconfined Compressive Strength were interesting. Earth blocks prepared with different types of raw materials exhibited significant differences in compressive strength values. Performances of clay-sand bricks could be improved by adding an optimum quantity of lime to reach the highest strength. Lime addition reduced the ability of compressed earth to absorb much water; thus, the density increased.

Obtained data suggest that potential use of representative clays as raw materials for manufacturing unfired clay blocks. In terms of mechanical properties, better results were given with clay A1, A2 and A3 respectively. A1 was located in the recommendation diagram according to NF XP P13-901 and then confirmed the plastic character. The geochemical analysis showed that the clay fraction had a ratio of SiO_2 / Al_2O_3 equal to 3. The SiO_2 content was 57.97% and the Al_2O3 was 18.71%. The high percentage of K_2O (6.38%) reveals the richness of clay in kaolinite (13.58%) and illite (25.7%). The percentage of CaO confirms the content of loss on ignition (5.07%).

Technological tests for bricks A1 stabilized with 10 % lime revealed a weight loss of 10.9%, a porosity of 6.31% and mechanical strength of 7.14 MPa.

Despite the low mechanical properties for soil A3, it is remediable to improve strength by granular corrections or adding some green additives.

References

[1] Oti J.E, Kinutihia J.M (2012) Stabilized unfired clay bricks for environmental and sustainable use. Appl.Clay Sci, Vol. 58, pp 52-59

[2] Muntohar A.S (2011) Engineering characteristics of the compressed stabilized earth bricks. CONSTR BUILD MATER, Vol.25, pp 4215-4220

[3] Gouny F, Fouchal F, Pop O, Maillard P, Rossignol S (2013) Mechanical behaviour of an assembly of wood-geopolymer-earth bricks. CONSTR BUILD MATER, Vol.38, pp 110-118

[4] El Fgaier F, Lafhaj Z, Antczak E, Chapiseau C (2016) Dynamic thermal performance of three types of unfired earth bricks. APPL THERM ENG, Vol.93, pp 377-383

[5] Morton T (2005) Unfired earth bricks building. Building for the future, pp 24-27

[6] Oti J.E, Kinuthia J.M, Bai J (2009) Compressive strength and microstructural analysis of unfired clay masonry bricks. Eng. Geology, Vol.109, pp 230-240

[7] Norme NFP 94-051 (1993) Reconnaissance et essais. Détermination des limites d'Atterberg. Limite de Liquidité à la coupelle. Limite de plasticité au rouleau

[8] GTR-LCPC (1987) Limites d'Atterberg, Limite de Liquidité, Limite de plasticité, Méthodes d'essai. LCPC, Vol.26

[9] Moore D.M, Reynolds Jr R.C (1997) X-Ray Diffraction and the Identification and Analysis of Clay Minerals. Second ed. Oxford Univ. Press, Oxford

[10] Lawrence M. A, David R. C (2015) Characterization and Analysis of Porosity and Pore Structures. Miner. Chem, Vol. 80, pp 61-164

[11] French-Standars-NFP-98-232-1 (1991). Tests relating to pavements- Determination of the Mechanical

[12] Agostino W. B, Domenico G, Céline P.B, Joao M, Nicolas S (2015) Briques de terre crue : procédure de compactage haute pression et influence sur les propriétés mécaniques

[13]AFNOR NF XP P13-901 (2001) Compressed earth blocks for walls and partitions: definitions Specifications – Test methods – Delivery acceptance conditions.

[14] AFNOR NF EN 933-1 (1997) Essais pour déterminer les caractéristiques géométriques des granulats - Partie 1 : détermination de la granularité. Analyse granulométrique par tamisage

[15] NF EN ISO 14688-1 (2003) Geotechnical investigation and testing – identification and classification of soil – part 1 : identification and description

[16] Delgado M.C.J, Guerrero I.C (2007) The selection of soils for unstabilised earth building: a normative review. CONSTR BUILD MATER, Vol.21, pp 237–251

[17] Cong M, Bing C, Longzhu C (2016) Variables controlling strength development of self-compacting earth-based construction. CONSTR BUILD MATER, Vol.123, pp 336-345

[18] Jamoussi F, Bédir M, Boukadi N, Kharbachi S, Zargouni F, Galindo A.L, Hélène P (2003) Clay mineralogical distribution and tectono-eustatic control in the Tunisian margin basins. Geosci, Vol.335, Issue 2, pp 175–183

[19] Brunauer S, Emmett P.H, and Teller E, (1938). Vol. *60* (2), pp 309–319

[20] Brunauer S, Emmett P. H, Teller E (1938) Adsorption of Gases in Multimolecular Layers. Contrib. Bur. Chem, Soils George Wash. Univ, Vol. 60, pp 309–319

[21] Aras A, (2004) The change phase composition in kaolinite and illite rich clay based ceramic bodies. Appl.Clay Sci 24, pp 257–269

[22] Farmer V.C (1968) Infrared spectroscopy in clay minerals study. CLAY MINER, Vol.7, pp 373–387

[23] Farmer V.C (1974) The infrared spectra of minerals. Mineral Sci, pp 331–365

[24] Russell J.D, Fraser A.R (1994) Infrared methods, Clay minerals: Spectroscopic and Chemical Determinative Methods. Chapman and Hall, London, pp 11–67

[25] Vander M.H.W, Beutels P.H (1976). Atlas Infrared Spectroscopy of Clay Minerals and their Admixtures

[26] Wheeler S. J, Sharma R. S, Buisson M. S. R (2003) Coupling of hydraulic hysteresis and stress–strain behaviour in unsaturated soils. https://doi.org/10.1680/geot.2003.53.1.41, GEOTECH, Vol.53, Issue1, pp 41-54

[27] Chiu F.C.W.W.Ng (2003) A state-dependent elasto-plastic model for saturated and unsaturated soils. https://doi.org/10.1680/geot.2003.53.9.809, GEOTECH, Vol. 53, Issue9, pp 809-829

[28] Jian W, Qimin L, Changwei Y, Yidan H.C (2018) A Simple Model for Elastic-Plastic Contact of Granular Geomaterials. ADV MATER SCI ENG, Vol. 2018, Article ID 6783791, https://doi.org/10.1155/2018/6783791

[29] Delebecque R (1990). Éléments de Construction Bâtiment, Edition Delagrave

[30] Guilaud H (1997) Centre International pour la Construction en Terre, Ecole d'Architecte de Grenoble, Encyclopédie de Bâtiment, Tome 2 Edition Wake, CRATerre.

[31] Rahmat M.N, Norsalisma I, Kinuthia J.M (2016) Strength and environmental evaluation of stabilized Clay-PFA eco-friendly bricks. CONSTR BUILD MATER, Vol.125, pp 964–973

[32]mechanical properties of fired-clay bricks incorporating ETP biosolids. Journal of Cleaner Production 119, http://dx.doi.org/10.1016/j.jclepro.2016.01.094

[33] El Fadaly E.A, El- Enany S.A (2015) Lead free Ceramic Cooking ware from Egyptian Raw Materials. I.J. current Microb. Appl Sci, ISSN: 2319-7706 Volume 4 Number 4, pp 474-487, http://www.ijcmas.com

[34] Simãoa L , Montedoa O.R.K, da Silva Paulaa M.M, da Silvaa L , Rafael Falchi Caldatob R.F, de Mello Innocentnib M.D (2013) Structural and Fluid Dynamic Characterization of Calcium Carbonate-based Porous Ceramics. Mater. Res, 16(6) : 1439-1448 © 2013 DDOI : 10.1590/S1516-14392013005000147

[35] Oti J.E, Kinuthia J.M (2012) Stabilized unfired clay bricks for environmental and sustainable use. Appl. Clay, pp 52–59

[36] Boussen S, Sghaier D, Chaabani F, Jamoussi B, Bennour A (2016) Characteristics and industrial application of the Lower Cretaceous clay deposits (Bouhedma Formation), Southeast Tunisia: Potential use for the manufacturing of ceramic tiles and bricks. Appl. Clay, Vol.123, pp 210-221

[37] Mahmoudi S, Bennour A, Meguebli A, Srasra E, Zargouni F (2016) Characterization and traditional ceramic application of clays from the Douiret region in South Tunisia. Appl. Clay Sci, Vol. 127-128, pp 78–87

[38] Riza F.V, Abdel Rahman I, Ahmad Zaidi A.M (2011) Possibility of lime as a stabilizer in compressed earth blocs (CEB). Int. J. Adv. Sci, Eng. Inf. Tech, Vol.1, Issue 6, pp 582-585

[39] Maskell D, Heath A, Walker P (2014) Inorganic stabilization methods for extruded earth masonry units. CONSTR BUILD MATER, Vol.71, pp 602–609

[40] Miqueleiz L, Ramírez F, Seco A, Nidzam R.M, Kinuthia J.M, Abu Tair A, Garcia R (2012) The use of stabilized Spanish clay soil for sustainable construction materials. Eng Geol, Vol. 133-134, pp 9–15

Figure captions

Fig. 1

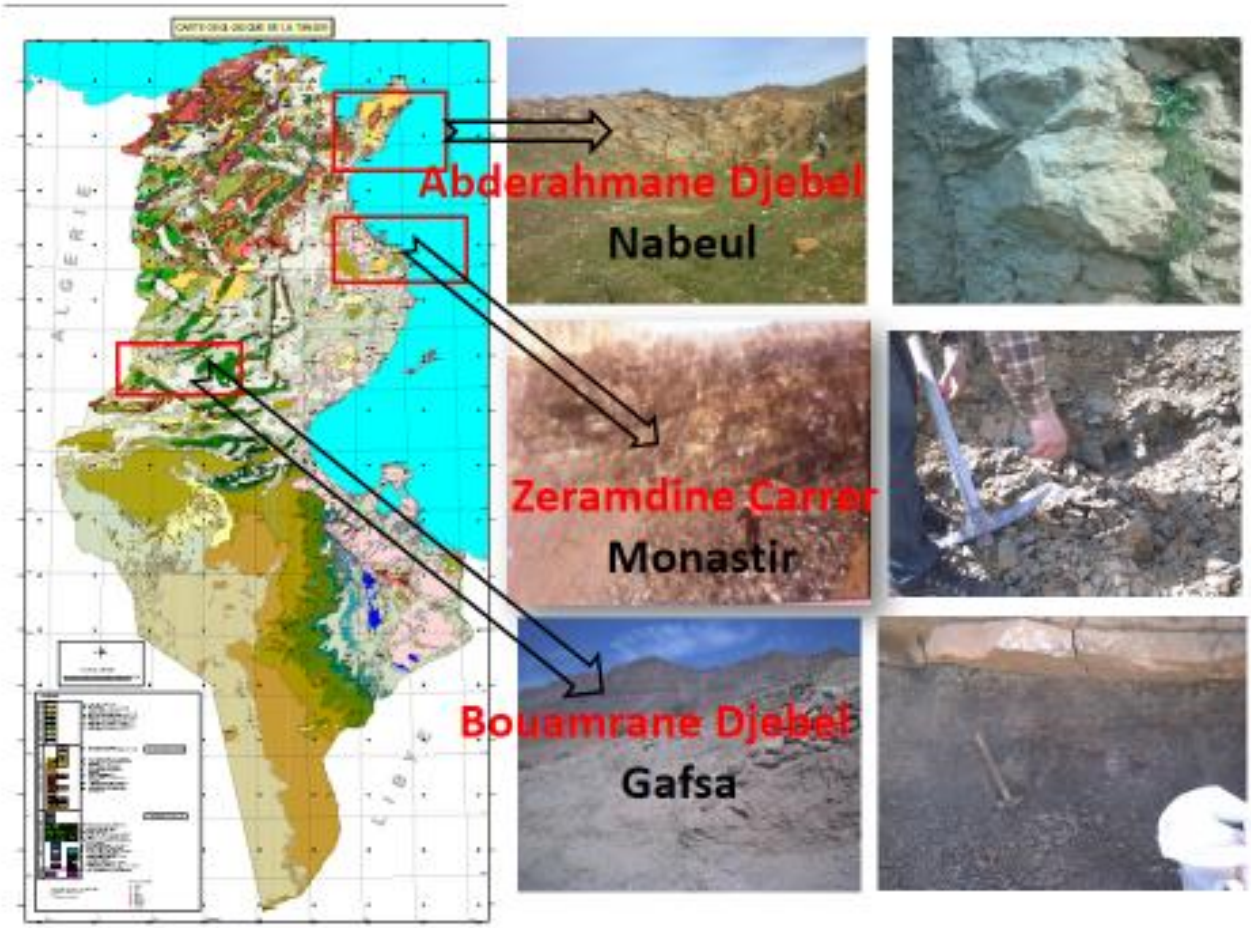
Abderahmane Djebel
Nabeul
Zeramdine Carrer
Monastir
Bouamrane Djebel
Gafsa

Fig. 2

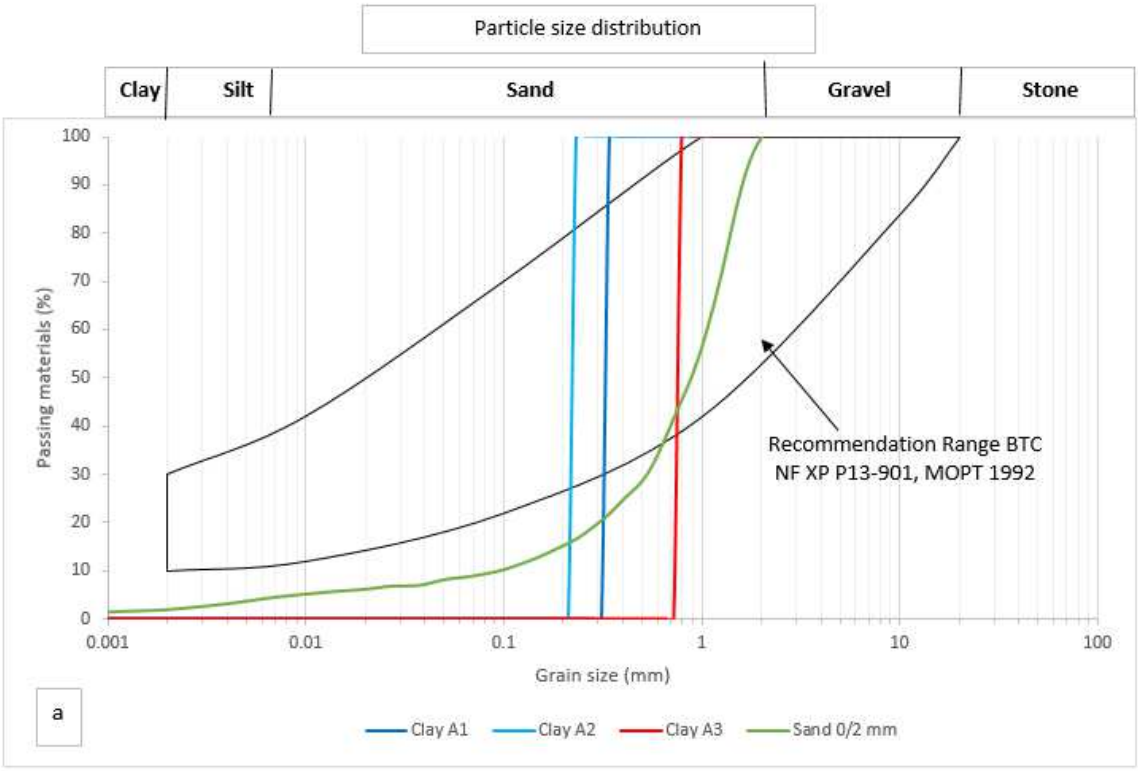
Particle size distribution
Clay
Silt
Sand
Gravel
Stone
Passing materials (%)
Grain size (mm)
Recommendation Range BTC
NF XP P13-901, MOPT 1992
a
Clay A1
Clay A2
Clay A3
Sand 0/2 mm

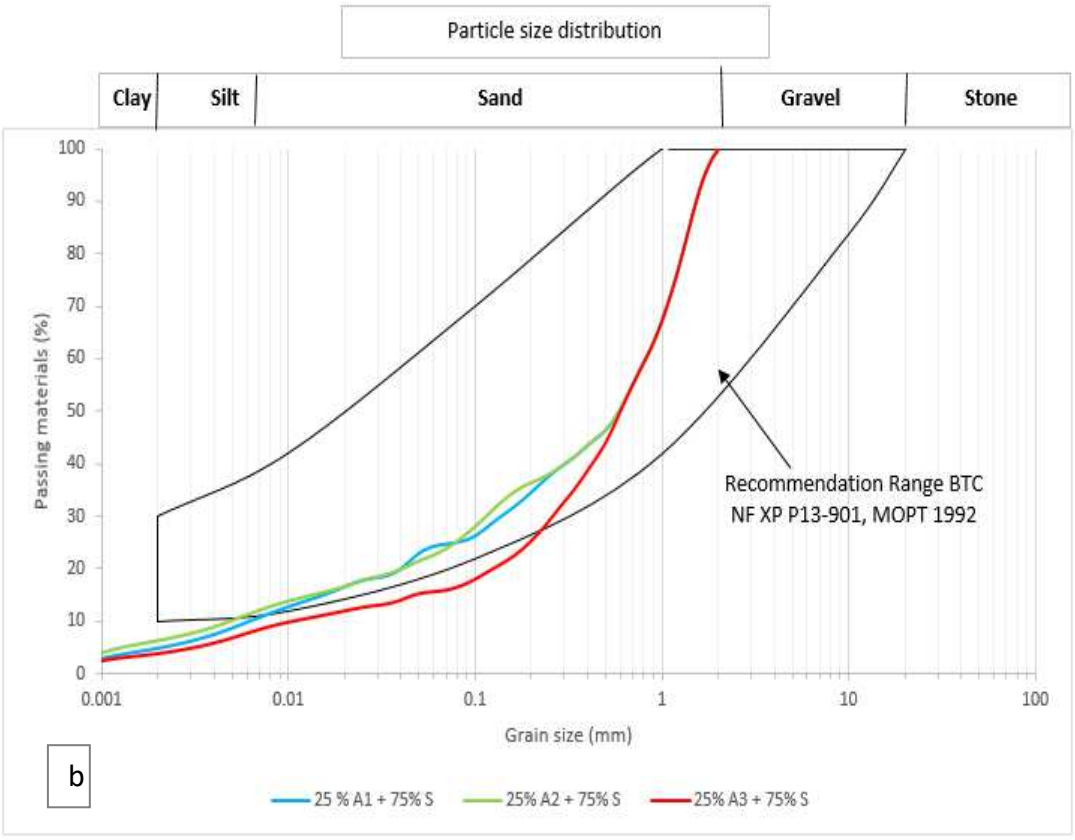
Particle size distribution
Clay
Silt
Sand
Gravel
Stone
Passing materials (%)
Grain size (mm)
Recommendation Range BTC
NF XP P13-901, MOPT 1992
b
25 % A1 + 75% S
25% A2 + 75% S
25% A3 + 75% S

Fig. 3

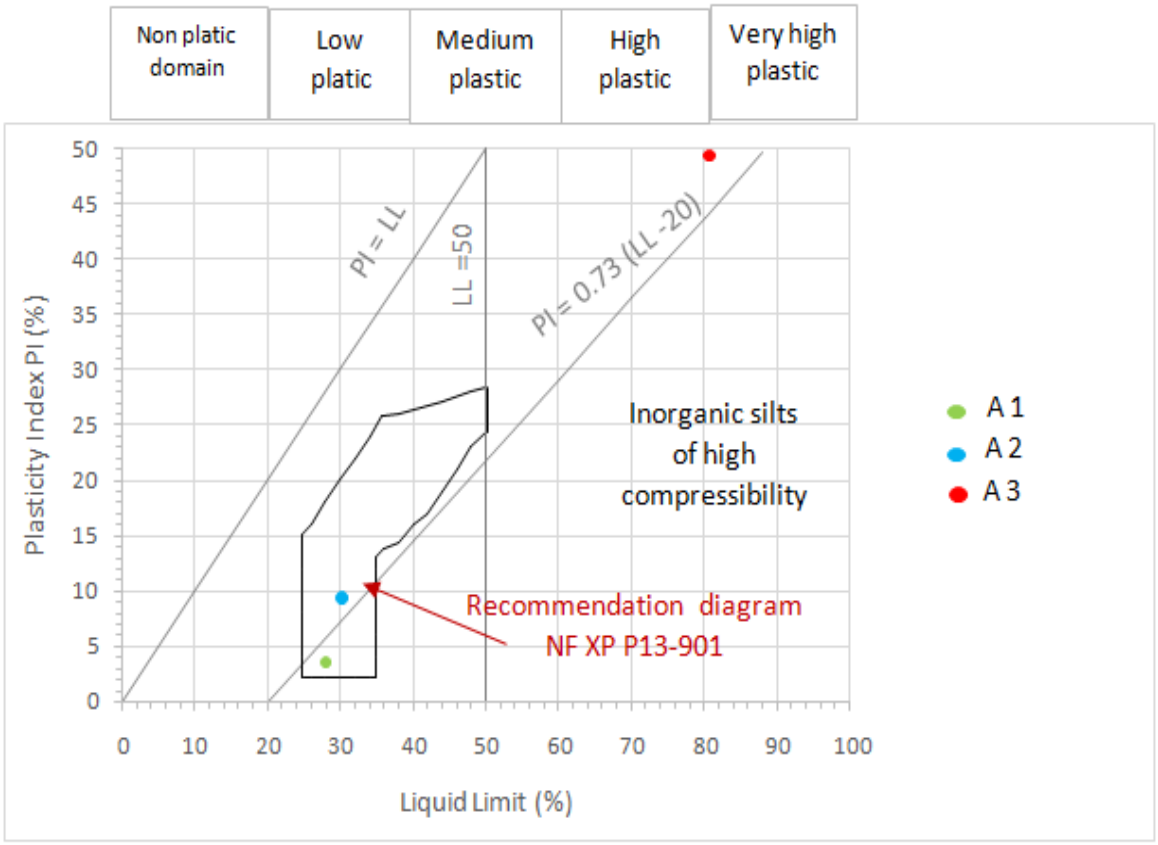
Non platic domain
Low platic
Medium plastic
High plastic
Very high plastic
Plasticity Index PI (%)
Liquid Limit (%)
PI = LL
LL =50
PI= 0.73 (LL -20)
Inorganic silts of high compressibility
Recommendation diagram NF XP P13-901
A 1
A 2
A 3

Fig. 4

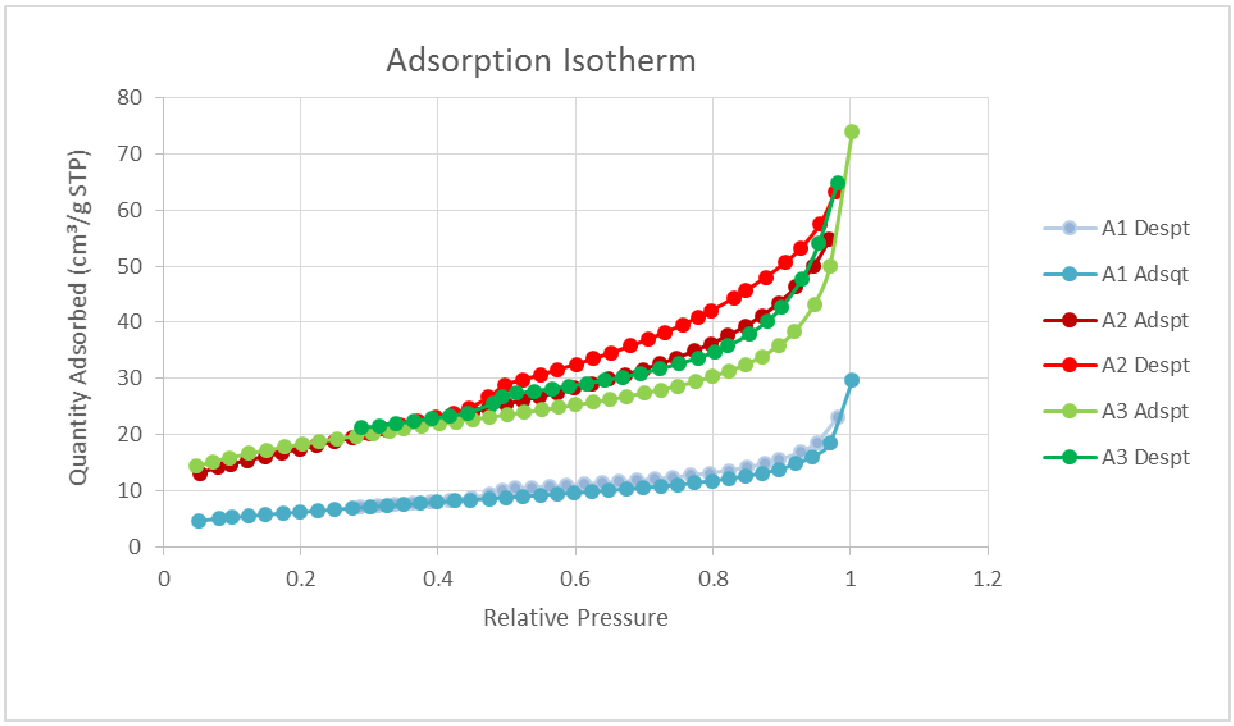
Adsorption Isotherm
Quantity Adsorbed (cm³/g STP)
80
70
60
50
40
30
20
10
0
0
0.2
0.4
0.6
0.8
1
1.2
Relative Pressure
A1 Despt
A1 Adsqt
A2 Adspt
A2 Despt
A3 Adspt
A3 Despt

Fig. 5

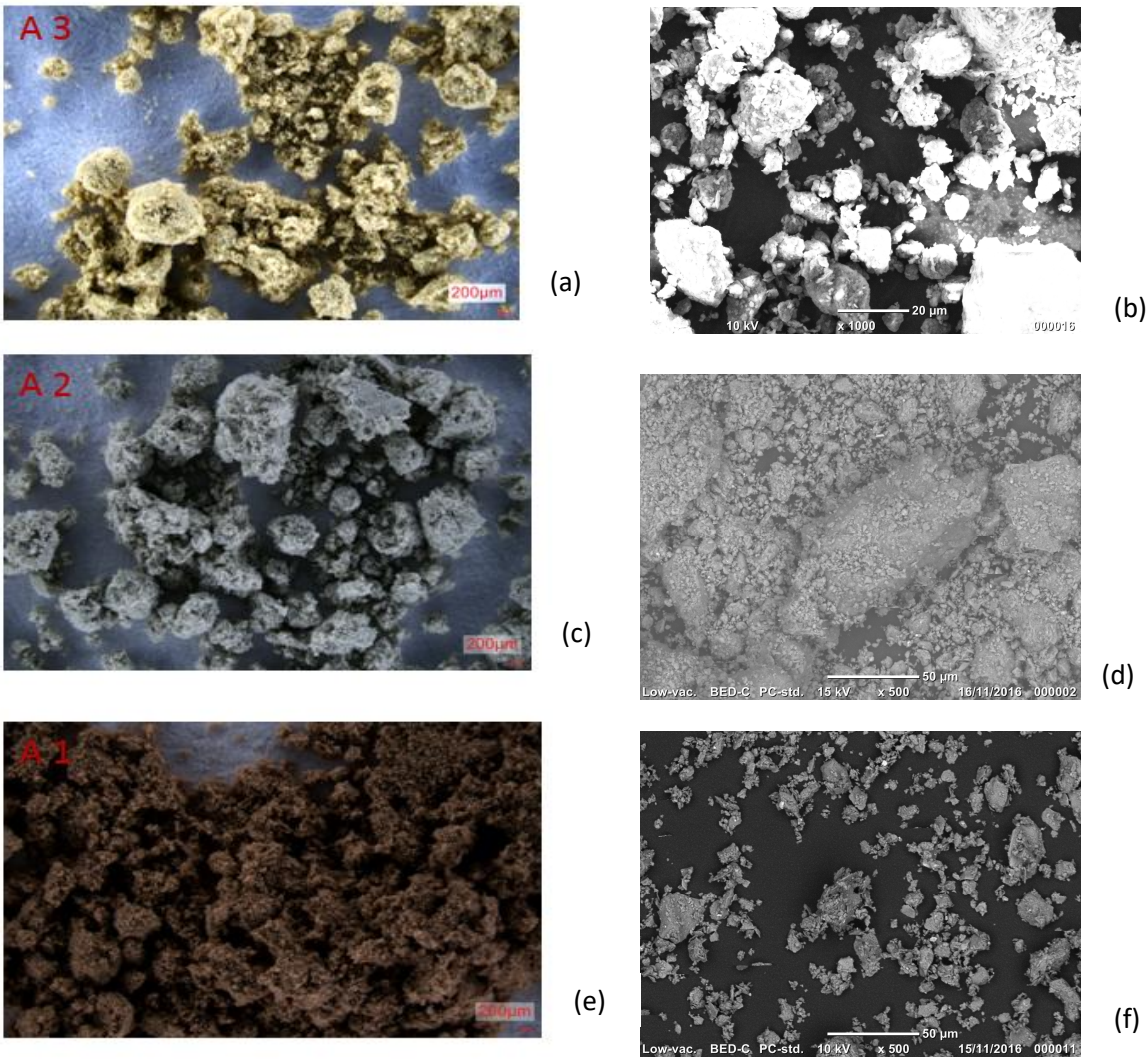
A 3
200µm
(a)
10 kV x 1000 20 µm 000015
(b)
A 2
200µm
(c)
Low-vac. BED-C PC-std. 15 kV x 500 50 µm 16/11/2016 000002
(d)
A 1
200µm
(e)
Low-vac. BED-C PC-std. 10 kV x 500 50 µm 15/11/2016 000011
(f)

Fig. 6

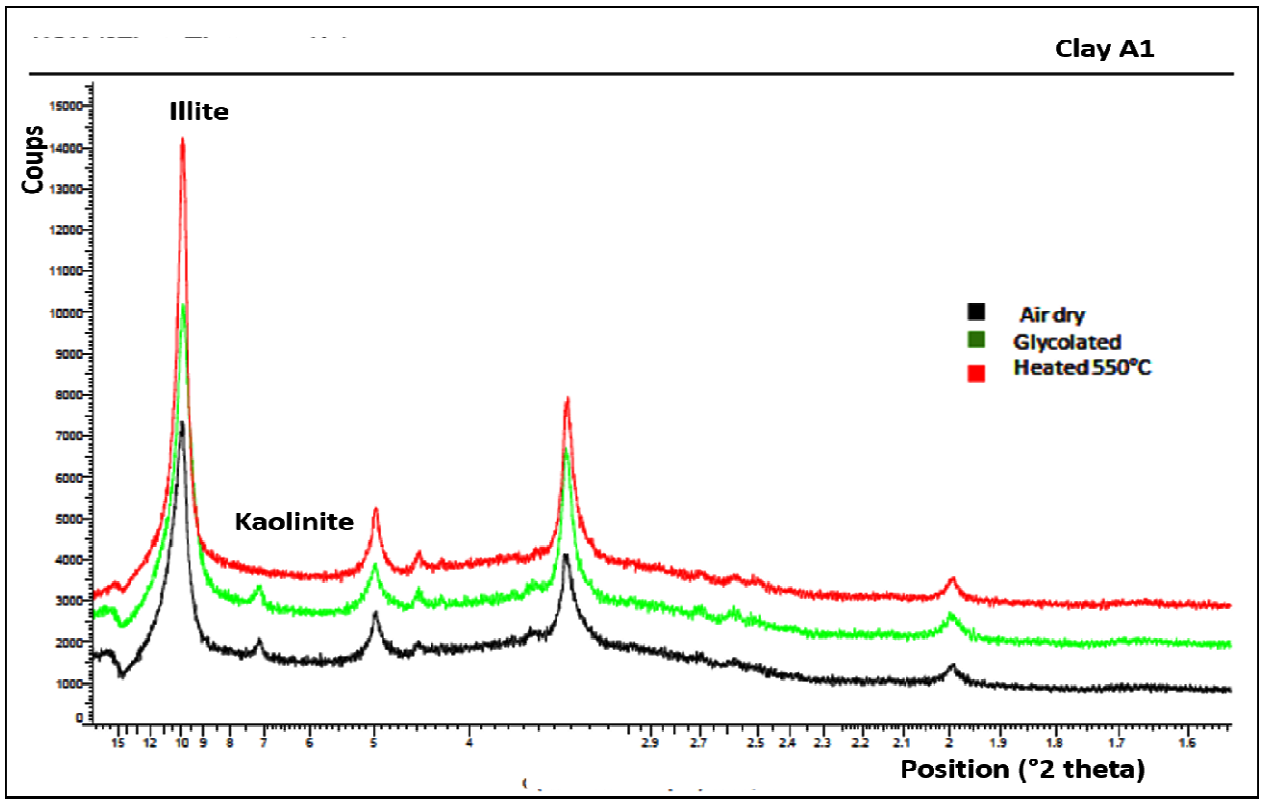
Clay A1
Illite
Kaolinite
Coups
Air dry
Glycolated
Heated 550°C
Position (°2 theta)

(a)

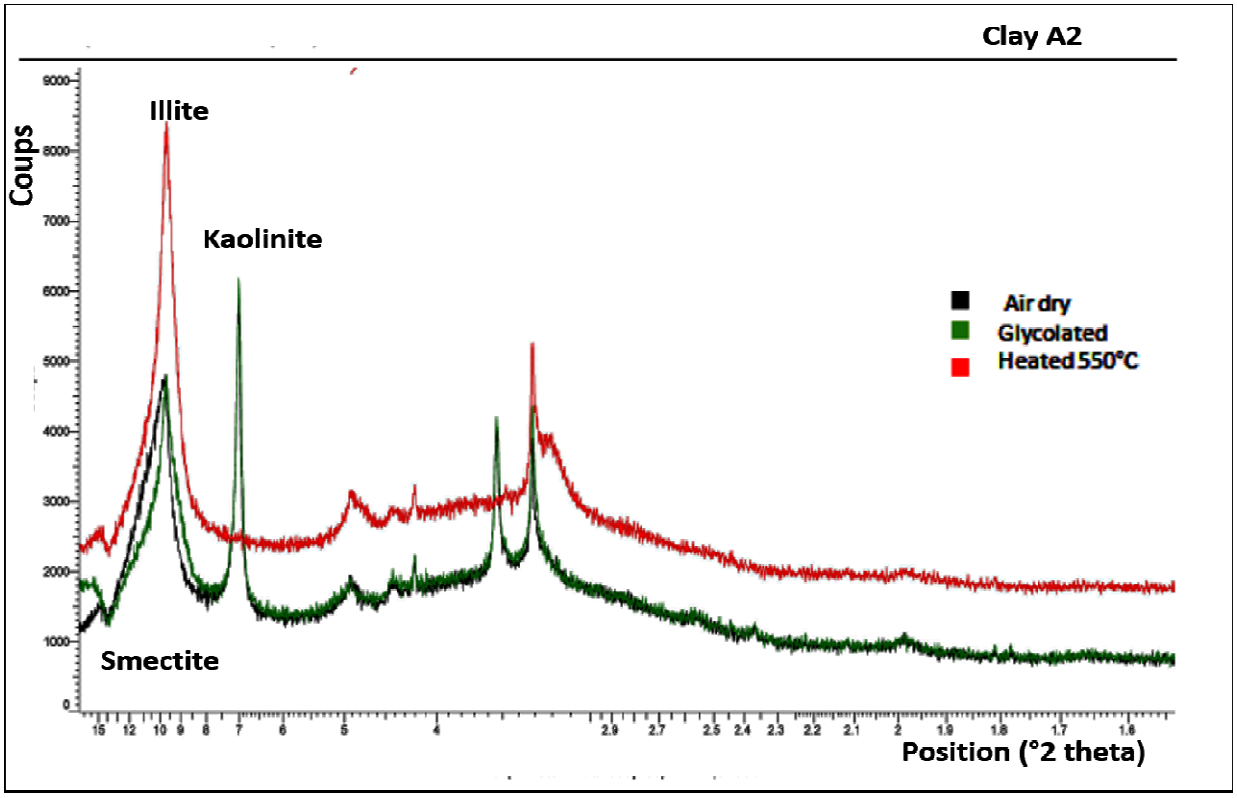
Clay A2
Illite
Kaolinite
Smectite
Coups
Air dry
Glycolated
Heated 550°C
Position (°2 theta)

(b)

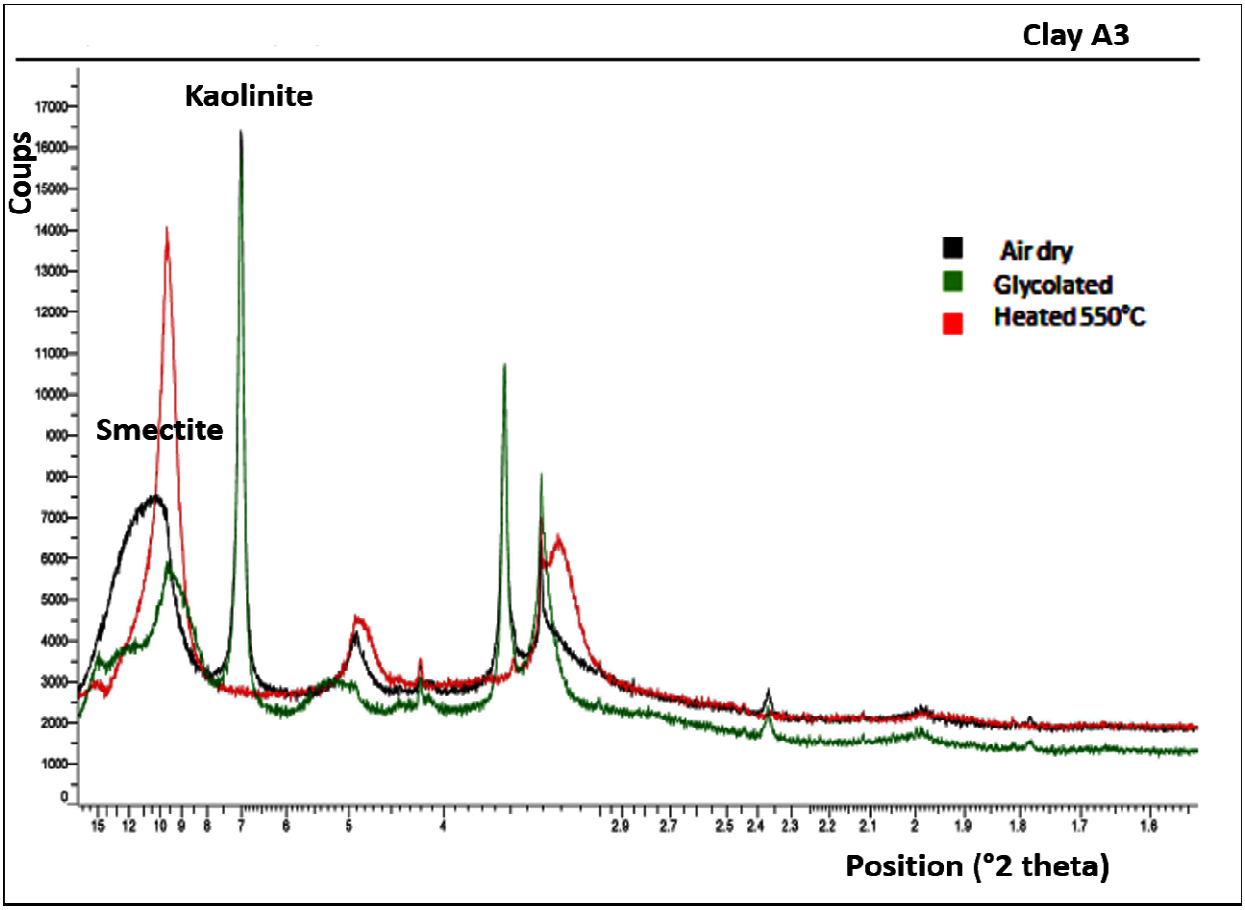
Clay A3
Kaolinite
Coups
Smectite
Air dry
Glycolated
Heated 550°C
Position (°2 theta)

(c)

Fig. 7

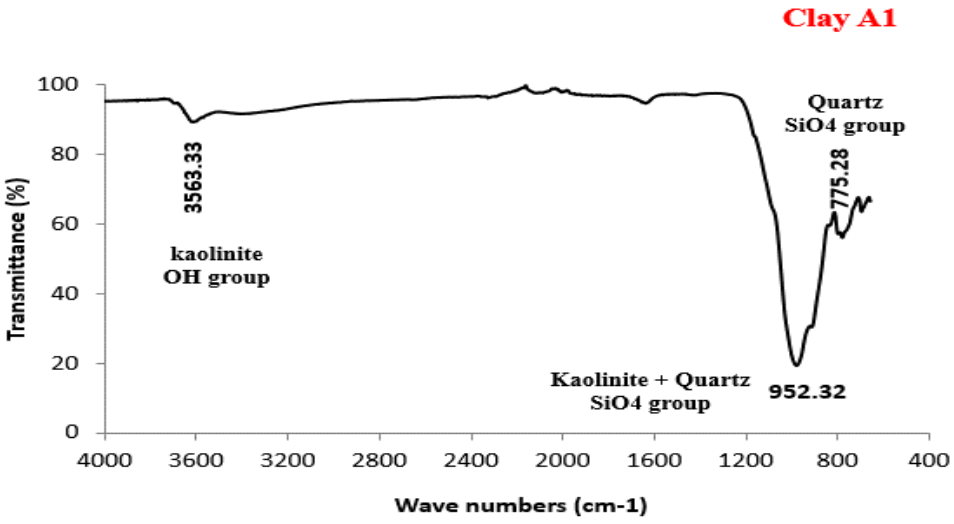
Clay A1
Transmittance (%)
Wave numbers (cm-1)
3563.33
kaolinite
OH group
Quartz
SiO4 group
775.28
Kaolinite + Quartz
SiO4 group
952.32

(a)

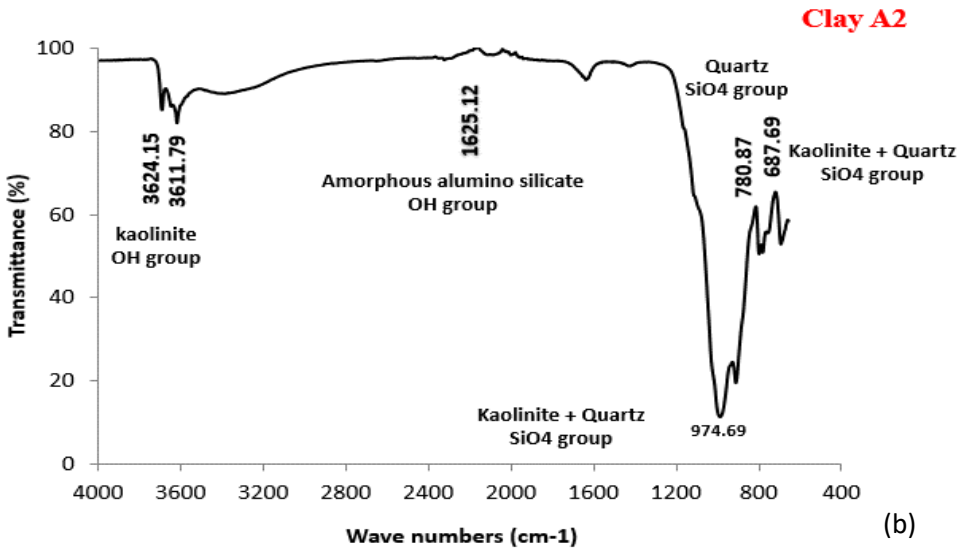
Clay A2
Transmittance (%)
Wave numbers (cm-1)
3624.15
3611.79
kaolinite
OH group
1625.12
Amorphous alumino silicate
OH group
Quartz
SiO4 group
780.87
687.69
Kaolinite + Quartz
SiO4 group
Kaolinite + Quartz
SiO4 group
974.69

(b)

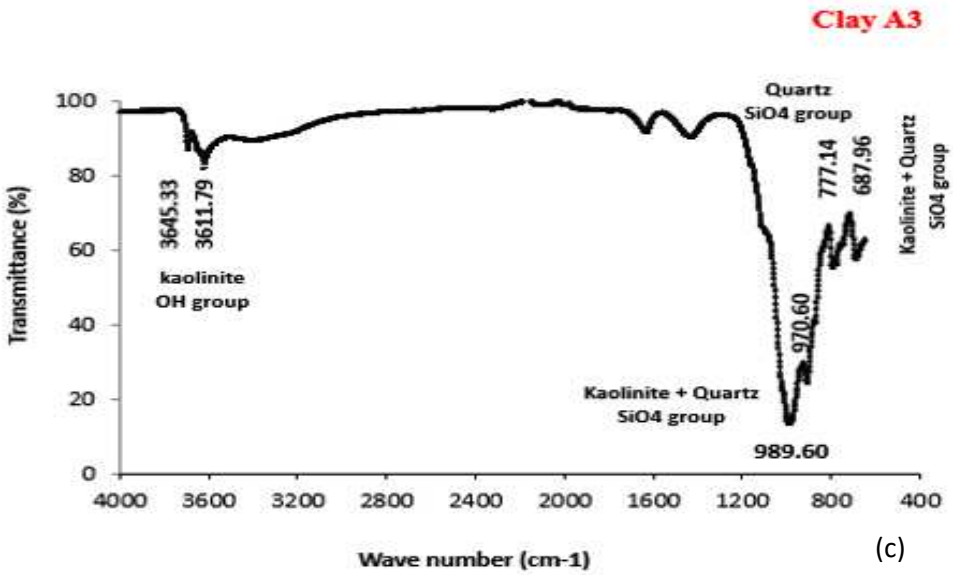
Clay A3
Transmittance (%)
Wave number (cm-1)
3645.33
3611.79
kaolinite
OH group
Quartz
SiO4 group
777.14
687.96
Kaolinite + Quartz
SiO4 group
970.60
Kaolinite + Quartz
SiO4 group
989.60

(c)

Fig. 8

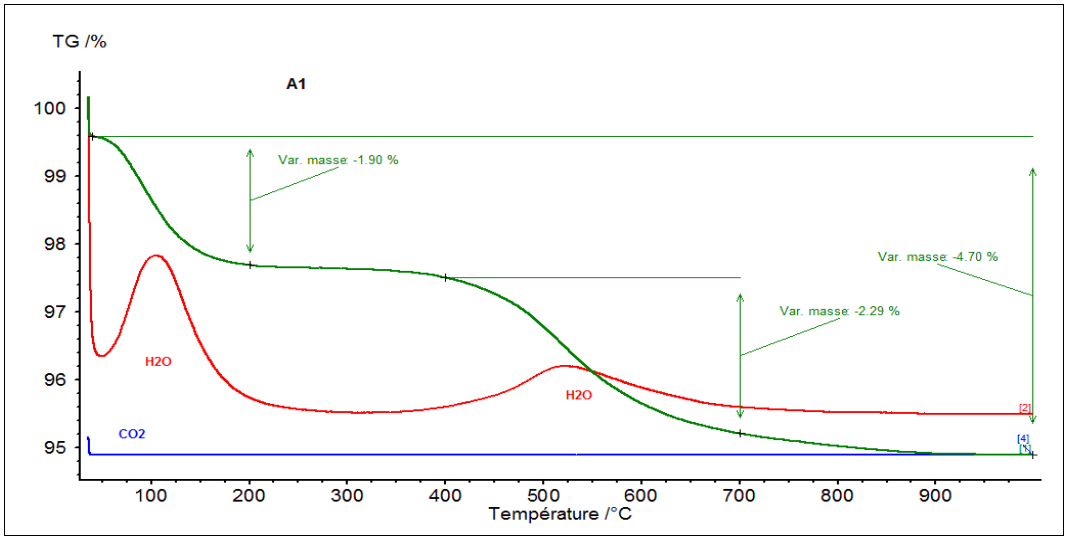
TG /%
A1
Var. masse: -1.90 %
Var. masse: -4.70 %
Var. masse: -2.29 %
H2O
H2O
CO2
Température /°C

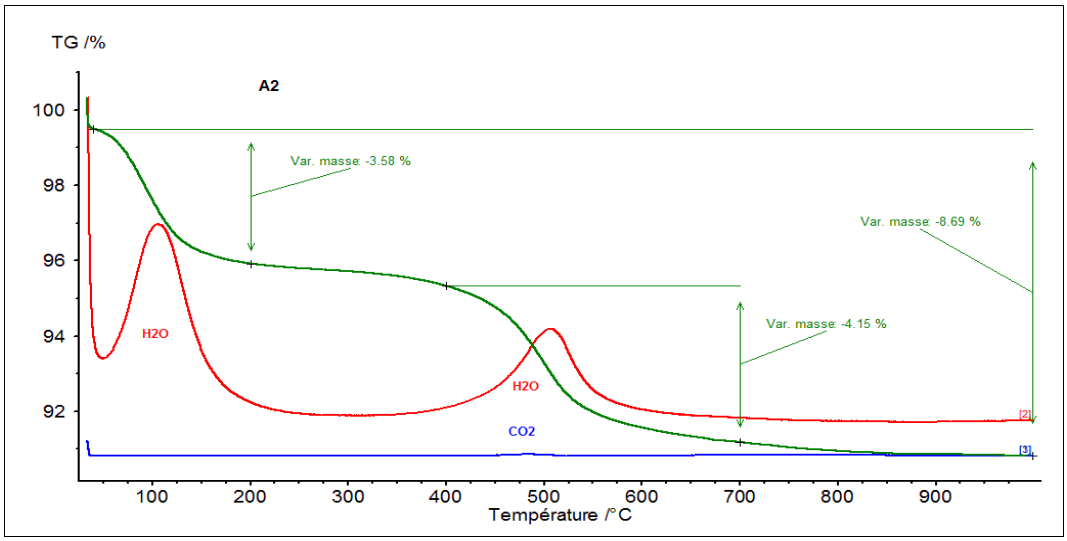
TG /%
A2
Var. masse: -3.58 %
Var. masse: -8.69 %
Var. masse: -4.15 %
H2O
H2O
CO2
Température /°C

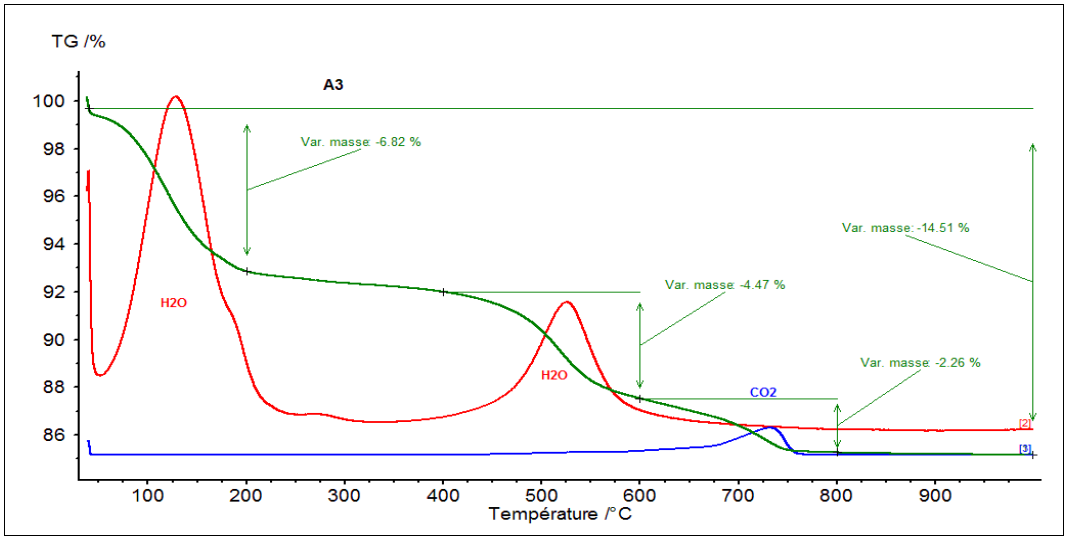
TG /%
A3
Var. masse: -6.82 %
Var. masse: -14.51 %
Var. masse: -4.47 %
Var. masse: -2.26 %
H2O
H2O
CO2
Température /°C

Fig. 9

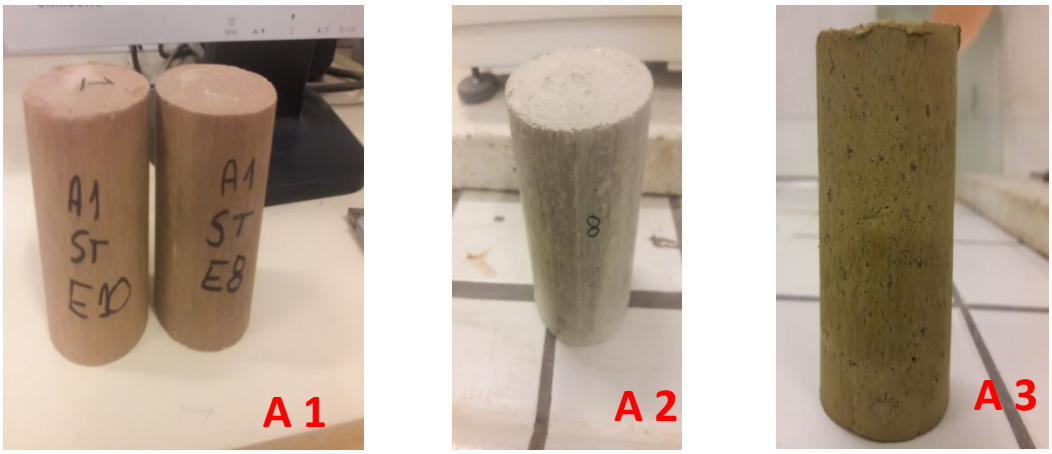

1 Fig. 10

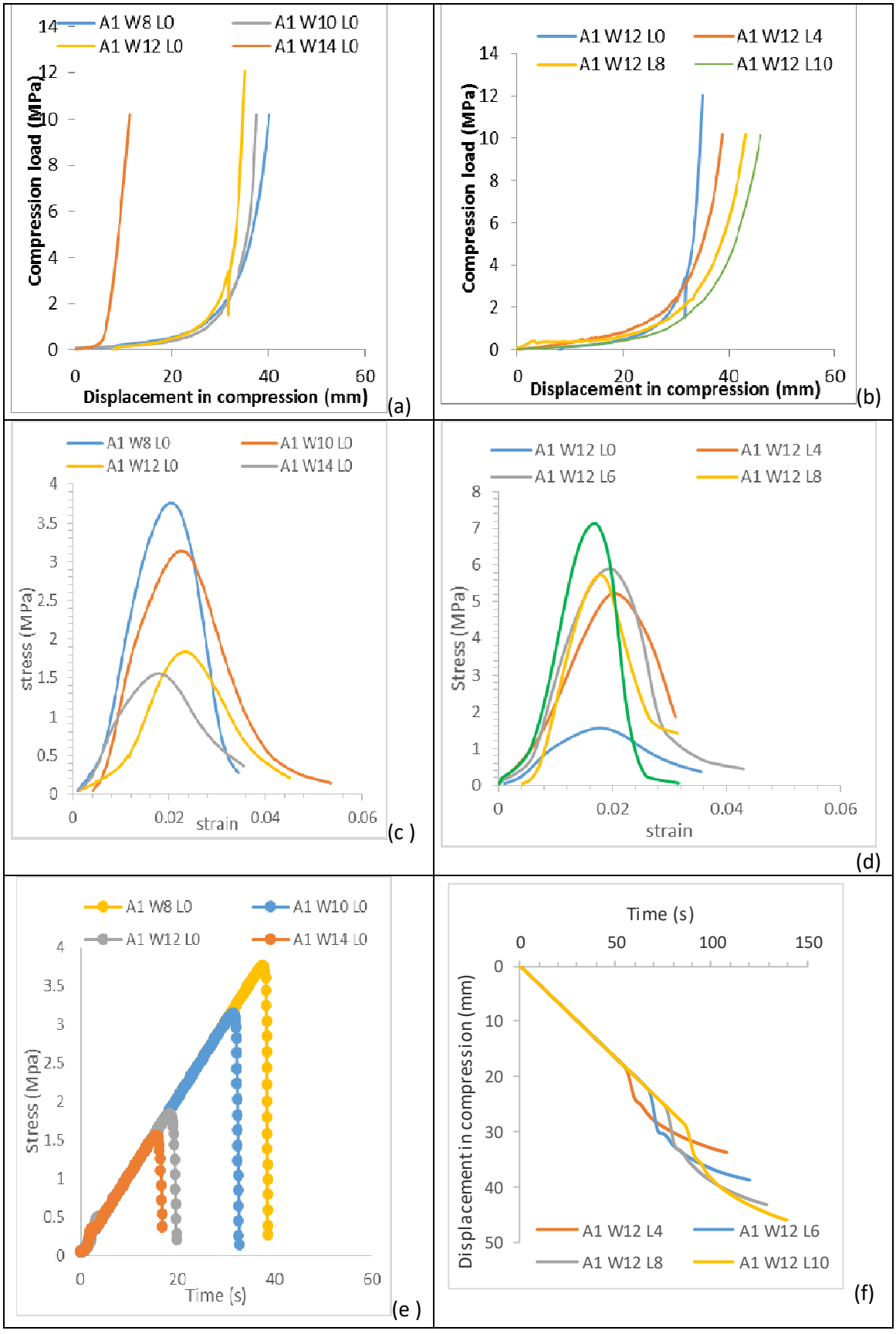
A1 W8 L0
A1 W10 L0
A1 W12 L0
A1 W14 L0
Compression load (MPa)
Displacement in compression (mm)
(a)
A1 W12 L0
A1 W12 L4
A1 W12 L8
A1 W12 L10
Compression load (MPa)
Displacement in compression (mm)
(b)
A1 W8 L0
A1 W10 L0
A1 W12 L0
A1 W14 L0
stress (MPa)
strain
(c)
A1 W12 L0
A1 W12 L4
A1 W12 L6
A1 W12 L8
Stress (MPa)
strain
(d)
A1 W8 L0
A1 W10 L0
A1 W12 L0
A1 W14 L0
Stress (Mpa)
Time (s)
(e)
Time (s)
Displacement in compression (mm)
A1 W12 L4
A1 W12 L6
A1 W12 L8
A1 W12 L10
(f)

2

1 Fig. 11

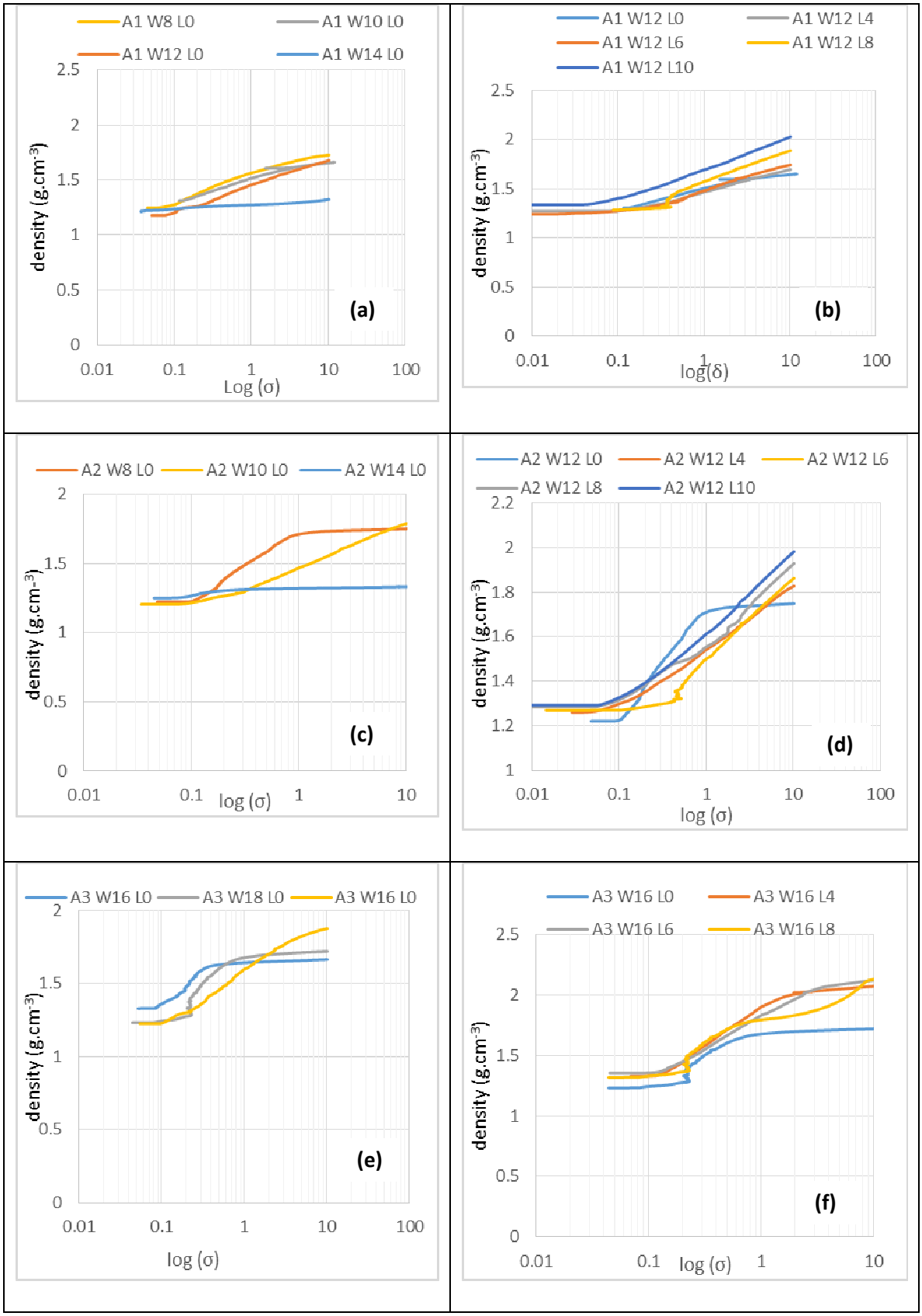
A1 W8 L0
A1 W10 L0
A1 W12 L0
A1 W14 L0
density (g.cm-3)
Log (σ)
(a)
A1 W12 L0
A1 W12 L4
A1 W12 L6
A1 W12 L8
A1 W12 L10
density (g.cm-3)
log(δ)
(b)
A2 W8 L0
A2 W10 L0
A2 W14 L0
density (g.cm-3)
log (σ)
(c)
A2 W12 L0
A2 W12 L4
A2 W12 L6
A2 W12 L8
A2 W12 L10
density (g.cm-3)
log (σ)
(d)
A3 W16 L0
A3 W18 L0
A3 W16 L0
density (g.cm-3)
log (σ)
(e)
A3 W16 L0
A3 W16 L4
A3 W16 L6
A3 W16 L8
density (g.cm-3)
log (σ)
(f)

2

1 Fig. 12

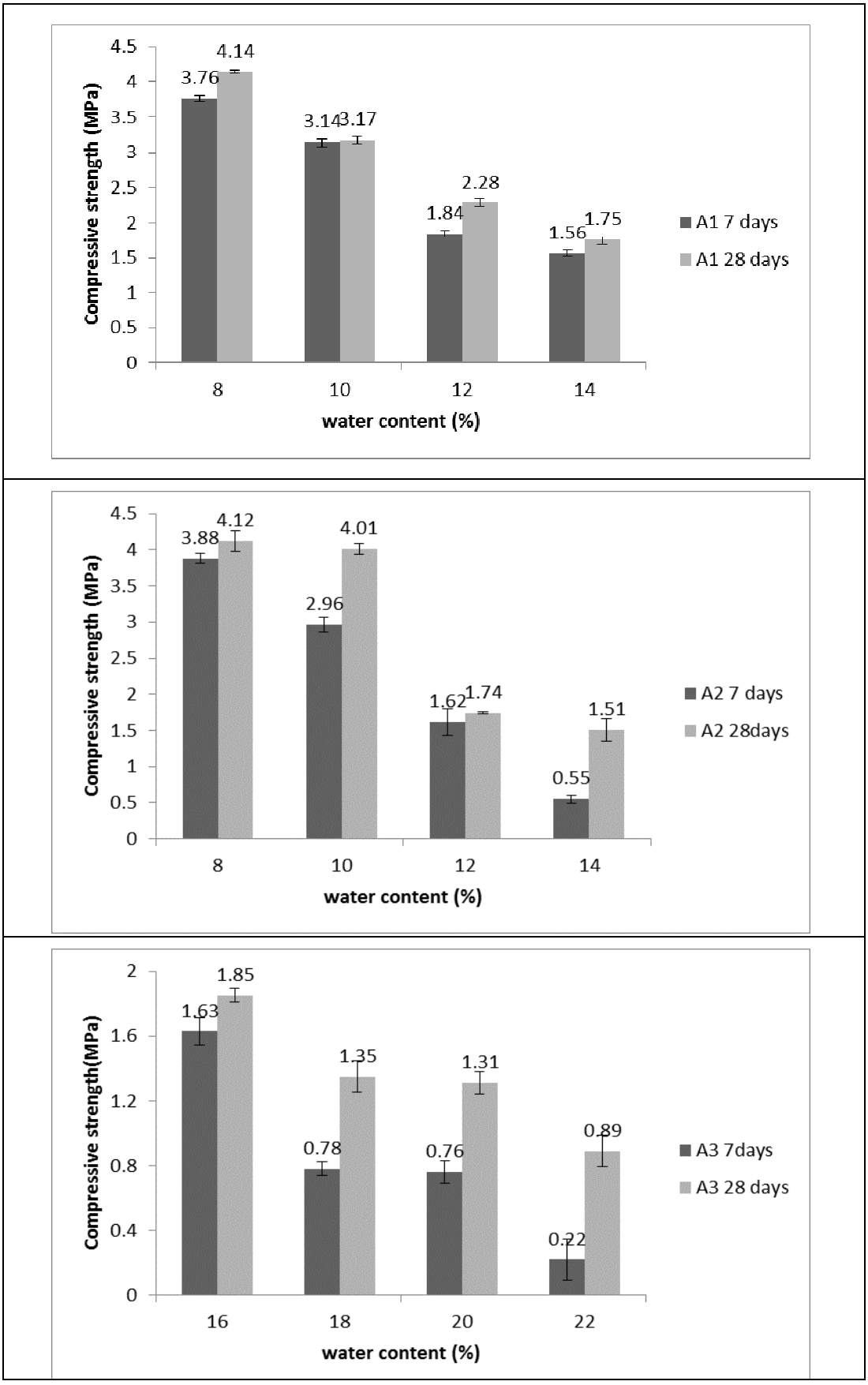
Compressive strength (MPa)
4.5
4
3.5
3
2.5
2
1.5
1
0.5
0
3.76
4.14
3.14
3.17
1.84
2.28
1.56
1.75
8
10
12
14
water content (%)
A1 7 days
A1 28 days
Compressive strength (MPa)
3.88
4.12
2.96
4.01
1.62
1.74
0.55
1.51
water content (%)
A2 7 days
A2 28days
Compressive strength(MPa)
2
1.6
1.2
0.8
0.4
0
1.63
1.85
0.78
1.35
0.76
1.31
0.22
0.89
16
18
20
22
water content (%)
A3 7days
A3 28 days

Fig. 13

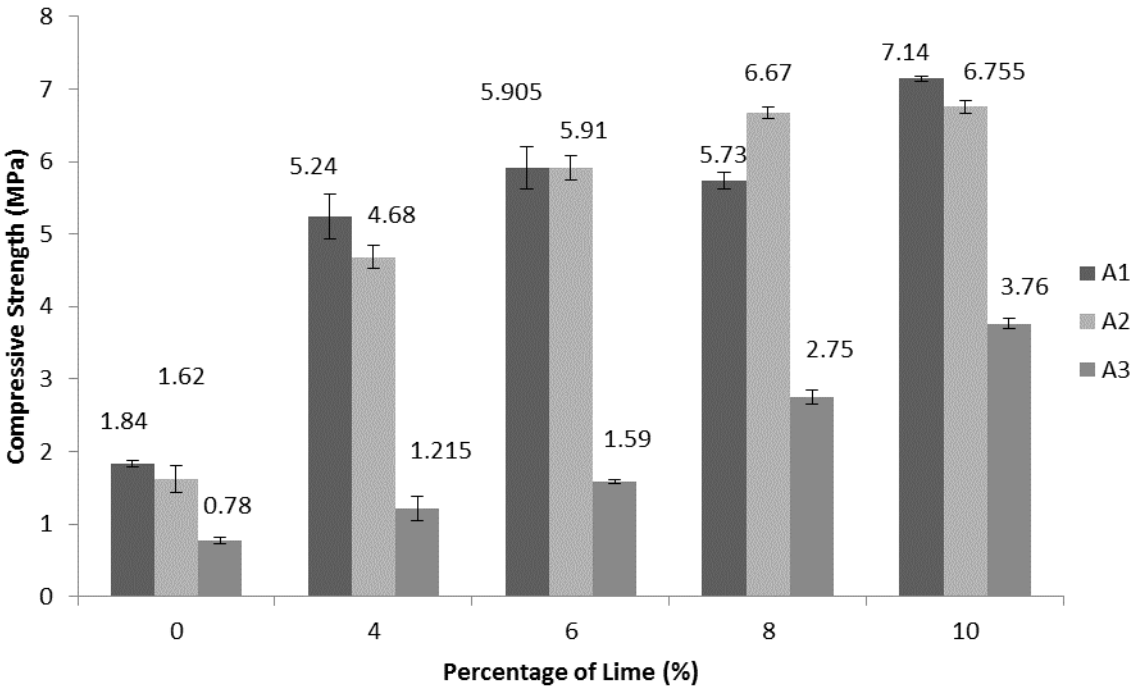
Compressive Strength (MPa)
Percentage of Lime (%)
0
4
6
8
10
1.84
1.62
0.78
5.24
4.68
1.215
5.905
5.91
1.59
5.73
6.67
2.75
7.14
6.755
3.76
A1
A2
A3

Table captions

Tab.1 Grain size of collected clays

Tab.2 Chemical analysis of studied clays (% by weight)

Tab.3 Formulas used

Tab.4 Values of Mass Loss for formulas studied

Tab.5 Porosity and packing density values

Tab. 6 Mixture composition effect

Table 1

samples	Clay (%)	Silt (%)	Sand (%)	d 10	d 30	d 60	C_u	C_c
A1	13.77	58.14	28.09	35.5	52.8	71.4	2.01	1.1
A2	19.62	46.48	33.9	41.1	53.6	65	1.58	1.08
A3	9.62	27.27	63.11	24.8	31.7	36.9	1.49	1.1
S	2.07	6.72	91.21	5.3	6.96	8.7	1.64	1.05

Table 2

Oxydes %	SiO_2	Al_2O3	Fe_2O_3	CaO	MgO	K_2O	Na_2O	TiO_2	SO_3	L.O.I	SiO_2/AL_2O_3
A1	57.97	18.71	6	0.42	2.32	6.38	0.94	1	0.12	5.07	3.09
A2	57.33	20.97	5.15	0.14	1.99	3.73	0.54	1	0.16	6.42	2.7
A3	51.77	20.78	5.29	3.78	2.16	2.53	0.27	1	0.13	12.24	2.5

Table 3

Formulations	Clay type	% Sand	% Clay	% Lime
F 1	A 1 A 2 A 3	70	30	0
F 2	A 1 A 2 A 3	75	25	0
F 3	A 1 A 2 A 3	65	35	0
F 4	A 1 A 2 A3	70	30	4
F 5	A 1 A 2 A 3	70	30	6
F6	A 1 A 2 A 3	70	30	8
F 7	A 1 A 2 A3	70	30	10

Table 4

Formulation	Loss mass (7 days)	Loss mass (28 days)	Drying shrinkage (%)
70S 30A1 8W	7.03	7.48	3.39
70S 30A1 10W	8.86	8.89	3.42
70S 30 A1 12W	8.94	9.18	3.75
70S 30A1 14W	9.71	9.79	3.9
70S 30A2 14W	8.9	8.97	4.2
70S 30A2 12W	8.79	8.91	3.8
70S 30A2 10W	8.69	8.74	3.56
70S 30A2 8W	8.66	8.69	3.38
70S 30A3 22W	13.36	13.39	4.68
70S 30A3 20W	13.33	13.36	4.24
70S 30A3 18W	13.26	13.28	4.13
70S 30A3 16W	12.02	12.12	4.11

a. Effect of water content and Setting time on samples studied

Formulation	Loss mass (%)	Drying shrinkage (%)
70S 30A1 12W 0L	8.94	3.75
70S 30A1 12W 4L	8.98	3.1
70S 30A1 12W6L	9.4	2.9
70S 30A1 12W 8L	9.9	2.36
70S 30A1 12W10L	10.9	2.33
70S 30A2 12W 0L	8.79	3.8
70S 30A2 12W4L	8.9	3.14
70S 30A2 12W 6L	9.6	2.82
70S 30A2 12W 8L	9.8	2.27
70S 30A2 12W 10L	10.1	2.11
70 S 30A3 18W 0L	13.26	4.11
70S 30A3 18W 4L	13.38	3.69
70S 30A3 18W 6L	13.5	3.49
70S 30A3 18W 8L	13.9	3.42
70S 30A3 18W 10L	13.93	3.16

b. Effect of lime added effect on samples studied

Table 5

Formulations	Porosity (%)	Packing density (%)
70S 30A1 8W	7.06	92.64
70S 30A1 10W	8.2	91.8
70S 30 A1 12W	8.3	91.7
70S 30A1 14W	8.86	91.14
70S 30A2 14W	8.62	91.38
70S 30A2 12W	8.60	91.4
70S 30A2 10W	7.88	92.12
70S 30A2 8W	7.86	92.14
70S 30A3 22W	17.12	82.88
70S 30A3 20W	15.73	84.27
70S 30A3 18W	12.94	87.06
70S 30A3 16W	10.93	89.07

a. Effect of water content effect on samples studied

Formulations	Porosity (%)	Packing density (%)
70S 30A1 10W	8.2	91.8
75S 25A1 10 W	8.67	91.30
65S 35A1 10W	8.33	91.67
70S 30A2 10W	7.88	92.12
75S 25A2 10W	9.67	90.03
65S 35A2 10W	9.58	90.42
70S 30A3 18W	12.94	87.06
75S 25A3 18W	14.05	85.95
65S 35A3 18W	14.57	85.43

b. Effect of mixture composition on samples studied

Formulations	Porosity (%)	Packing density (%)
70S 30A1 12W 0L	8.3	91.7
70S 30A1 12W 4L	7.81	92.19
70S 30A1 12W 6L	6.52	93.48
70S 30A1 12W 8L	6.33	93.67
70S 30A1 12W 10L	6.31	93.69
70S 30A2 12W 0L	8.60	91.4
70S 30A2 12W 4L	8.42	91.58
70S 30A2 12W 6L	7.85	92.15
70S 30A2 12W 8L	7.82	92.18
70S 30A2 12W 10L	7.32	92.68
70 S 30A3 18W 0L	12.94	87.06
70S 30A3 18W 4L	12.2	87.7
70S 30A3 18W6L	10.21	89.79
70S 30A3 18W 8L	9.17	90.83

c. Effect of lime added on samples studied

Table 6

Clay type	% Clay	% Sand	Compressive strength (MPa)
A 1	25	75	2.68
A 1	30	70	3.14
A1	35	65	2.87
A 2	25	75	0.59
A 2	30	70	2.96
A 2	35	65	1.19
A 3	25	75	0.69
A 3	30	70	0.78
A 3	35	65	0.68